is determined. Because the ultrasonic propellant burner is a closed vessel, the burning rates can be correlated with the increasing burner pressure.

Results and Discussion

Figure 1 shows the ballistic results for propellants 1, A, and B. The burning rates show no significant alteration among the three propellants. The differential scanning calorimetry plots for these three propellants shown in Fig. 2 tell a different story, however. Compared with the baseline, both the carbon and the fullerene soot appear to eliminate the secondary exothermic peak at approximately 275°C. Both also seem to have exothermic activity centered around the BTTN/TMETN exotherm at 200°C. The existence of the double exotherms for the soot propellant B (-071) as opposed to the single exotherm for the carbon black propellant A (-028) can be accounted for by recalling that the fullerene soot contains a variety of carbon molecular forms, with different structures and volatilities.

Examination of the optical microscope photographs of the extinguished surfaces of the two modified propellants also revealed a substantial change from the baseline. The surfaces for propellants A (-028) and B (-071) were dry, with no evidence of the AN melt layer noted in propellant 1 (baseline). Based on the absence of the second exotherm for propellants A and B, it is evident that the exotherm is due to a reaction between BTTN/TMETN decomposition products and the AN melt layer. This is supported by the fact that, in the baseline propellant, which has a thick melt layer, the second exotherm shows a sharp drop at ~270°C, corresponding to the rapid drop of the vaporization endotherm for the AN melt. If the melt layer is eliminated, then so is the exotherm.

From a purely qualitative standpoint, the trade of carbon and fullerene soot for the nitrate esters has a substantial effect on the condensed-phase behavior and surface morphology of the AN propellant compared to the baseline. However, no measurable effect is evident in terms of burning rate behavior, or dominance of the flame kinetics over diffusion mechanisms. There are two possible reasons for this behavior: 1) The gas-phase energy release dominates any condensed-phase contribution to the overall chemical energy release or 2) any benefit gained from carbon or fullerene enhancement of AN combustion is masked by elimination of the second exotherm when the BTTN/TMETN is reduced. What is clear is that for this propellant/binder system, elimination of the melt layer or changes in the condensed phase reactions do not significantly alter the ballistics. Additionally, although the fullerene soot has a different effect than carbon on the condensed-phase behavior of the AN/BTTN/TMETN propellant when exchanged for the plasticizer, its effect is not substantially different from carbon on the propellant ballistics.

References

[1]Billheimer, J. S., Brown, C. O., and Brown, L. H., "Low-Cost-Propellant Development Program," Aerojet Engineering Corp., Sacramento, CA, Program Rept. 1098/99-2, 31 Dec. 1951.

[2]Clarke, R. P., King, S. M., and Calcote, H. F., "Methods of Increasing the Burning Rate of Ammonium Nitrate Solid Rocket Propellants," Experiment Inc., Final Rept. AF 33 (038)-21837, June 1952.

[3]Glazkova, A. P., Kazarova, Y. A., and Savel'ev, A. V., "Oxidation of Carbon by Nitrates and Nitrites," *Fizika Goreniya I Vzryva*, Vol. 19, No. 3, 1983, pp. 65–73 (translation).

[4]Jain, S. R., and Oommen, C., "Thermal Ignition Studies on Metallized Fuel-Oxidizer Systems," *Journal of Thermal Analysis*, Vol. 35, 1989, pp. 1119–1128.

[5]Talley, S. K., and Miles, T. K., "Improvement of Burning Rate of Solid Propellants by Use of Stiffening Agents," *JANNAF 10th Meeting Bulletin*, Vol. 1, June 1954, pp. 279–290.

[6]Greiner, B. E., and Frederick, R. A., "Experimental Investigation of Ammonium Nitrate Propellant Ballistics Properties," AIAA Paper 96-3275, July 1996.

[7]Cauty, F., Démarias, J.-C., and Iradés, C., "Determination of Solid Propellant Burning Rate to the Initial Temperature by the Ultrasonic Method," Non-Intrusive Combustion Diagnostics, edited by K. K. Kuo and T. P. Parr, Begell House, Inc., New York, 1994.

[8]Di Salvo, R., Dauch, F., Frederick, R. A., Jr., and Moser, M. D., "Direct Ultrasonic Measurement of Solid Propellant Ballistics," *Review of Scientific Instruments*, Vol. 70, No. 11, 1999, pp. 4416–4421.

Performance Analysis of Short Takeoff and Vertical Landing Aircraft Nozzle in Hover

Frank K. Lu*
University of Texas at Arlington, Arlington, Texas 76019
and
Douglas A. Terrier†
Lockheed Martin Aeronautics Company, Fort Worth, Texas 76101

Nomenclature

A	=	cross-sectional area
k	=	specific heat ratio
M	=	Mach number
$\dot{m}$	=	mass flux
P	=	pressure
q	=	dynamic pressure
R	=	gas constant
T	=	temperature
V	=	velocity

Subscripts

t	=	total
0	=	far upstream
8	=	nozzle throat
9	=	nozzle exit

Introduction

FOR the propulsion system of a short takeoff and vertical landing (STOVL) vehicle such as the F-35 joint strike fighter (JSF), good propulsive efficiency[1] at high speeds dictates a high-velocity thrust stream, whereas efficient hover operation is achieved by propelling a large mass of low-speed air. The exhaust flow conditions in hover are radically different from those in transonic acceleration; however, the nozzle provides the same flowpath for both (Fig. 1). The F-35 nozzle is scheduled to provide an internal expansion ratio of 1.3 to give good performance for transonic acceleration. This nozzle expansion ratio is also presented in hover that produces overexpansion, resulting in significant thrust loss. For the three important mission points of transonic cruise, acceleration, and hover, the nozzle pressure ratio (NPR) are 3–4, 6–8, and 2, whereas the respective exhaust temperatures are 780, 2000, and 780 K.

Nozzle Performance Analysis

The nozzle gross thrust

$$F_g = \dot{m}V_9 + (P_9 - P_0)A_9 \tag{1}$$

is maximized when the flow is expanded to ambient pressure, this being governed by the nozzle geometry. Cruise produces a cool,

Presented as Paper 2003-0184 at the 41st Aerospace Sciences Meeting and Exhibit; received 3 December 2002; revision received 31 March 2003; accepted for publication 4 April 2003.

*Professor, Mechanical and Aerospace Engineering Department, and Director, Aerodynamics Research Center. Associate Fellow AIAA.

†Senior Manager, International Business Development; currently Office of Business Development, Building 1229, MS 200, NASA Langley Research Center, Hampton, VA 23681.

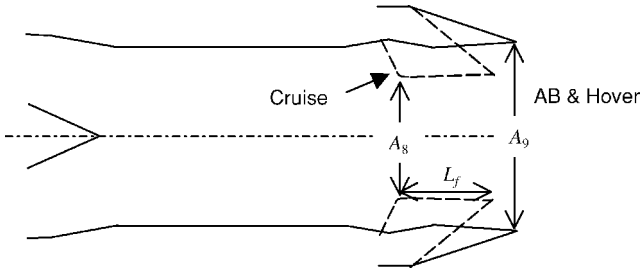

Fig. 1 JSF convergent–divergent nozzle: – – –, cruise configuration.

high-density exhaust flow, whereas afterburning produces a hot, low-density exhaust flow. Thus, the nozzle has variable geometry to accommodate the different engine operating conditions. The necessity for a variable throat area is readily seen from the continuity equation, which can be expressed in terms of the choked nozzle throat conditions as

$$\dot{m} = \rho_8 V_8 A_8 = p_8 A_8 \sqrt{k/(RT_8)} \tag{2}$$

Mass flow and pressure may be assumed to be roughly equal at afterburning and nonafter-burning conditions. However, there is a dramatic difference in temperature due to the additional fuel flow in afterburner operation. Equation (2) shows that A_8 must vary directly with $\sqrt{T_8}$ to maintain constant mass flow.

Whereas the throat area primarily governs mass flow characteristics, the divergent section geometry largely governs nozzle thrust efficiency, expressed by the gross thrust coefficient

$$C_{fg} = F_g \Big/ \left(\dot{m} M_{\mathrm{id}} \sqrt{kRT_9}\right) \tag{3}$$

where the ideal Mach number is

$$M_{\mathrm{id}} = [2/(k-1)]\left[\mathrm{NPR}^{(k-1)/k} - 1\right] \tag{4}$$

and the nozzle exit temperature is

$$T_9 = T_t\{1 + [(k-1)/2]M_{\mathrm{id}}\}^{-2} \tag{5}$$

For first-order analysis, C_{fg} may be decomposed into three subcoefficients as follows:

$$C_{fg} = C_{\mathrm{exp}} C_{\mathrm{div}} C_{\mathrm{vel}} \tag{6}$$

where

$$C_{\mathrm{exp}} = [\dot{m} M_9 kRT_9 + (P_9 - P_0)A_9]/F_{id} \tag{7}$$

is the expansion coefficient that accounts for losses due to under- or overexpansion of the flow due to nonoptimum nozzle area ratio, C_{div} is the coefficient of divergence loss resulting from nonaxial exit flow, and C_{vel} is the velocity coefficient accounting for friction along the nozzle wall. The divergence loss is found by integrating the area-averaged exit plane discharge angle. When a radial flow pattern is assumed,

$$C_{\mathrm{div}} = (1 + \cos\theta)/2 \tag{8}$$

where θ is the nozzle wall divergence angle. The friction loss coefficient is obtained by integrating the local skin friction over the nozzle surface. A constant value of the local skin-friction coefficient $c_f = 0.005$ is assumed for simplicity. The total friction is obtained by taking the sum of local values calculated for discrete zones along the nozzle. Therefore,

$$C_{\mathrm{vel}} = 1 - \sum_{j=1}^{J} \frac{q_j A_j c_f}{F_{\mathrm{id}}} \tag{11}$$

where

$$q_j = 0.7 M_j p_j \tag{12}$$

and A_j are the local dynamic pressure calculated at each zone and the surface area of the zone, respectively. In Eq. (12), M_j and p_j are evaluated using

$$A_j/A_8 = (1/M_j)\left([2/(k+1)]\left\{1 + [(k-1)/2]M_j^2\right\}\right)^{(k+1)/[2(k-1)]} \tag{13}$$

$$p_j = p_t\left[1 + 0.5(k-1)M_j^2\right]^{-k/(k-1)} \tag{14}$$

Experiment Method

To support the analysis, a 12% JSF nozzle was tested with cold air in the Lockheed Martin Aeronautics Company Thrust Measurement Facility.[2] This facility consists of a six-component thrust stand housed in an altitude chamber. Data repeatability is better than ±0.25%, whereas the error in C_{fg} is less than ±0.2%. The tests were conducted at a constant nozzle total pressure of 83 kPa, giving a Reynolds number of 5×10^6 based on throat diameter. This Reynolds number is an order of magnitude lower than full-scale conditions but, nonetheless, was found to provide adequate simulation of important nozzle flow phenomena.[2] The NPR = 2–6 to cover conditions from hover to transonic acceleration.

Results and Discussion

The predicted values of C_{fg} as a function of NPR for various A_9/A_8, where the throat areas of 0.290 and 0.484 m^2 represent the cruise and transonic acceleration or hover conditions, respectively, are shown in Fig. 2. The results display the main characteristics typical of nozzle thrust performance.[3] For a given A_9/A_8, C_{fg} peaks and then falls off with increasing NPR. Peak thrust occurs at a higher NPR for larger A_9/A_8. The peak value of C_{fg} is generally lower for higher A_9/A_8. For a given A_9/A_8, peak C_{fg} occurs at the NPR where the flow is fully expanded to ambient pressure. At lower NPR, the flow expands to an exit Mach number governed by A_9/A_8, producing a subambient exit pressure, which leads to a thrust loss at hover. Conversely, at higher NPR, P_9 is above ambient,

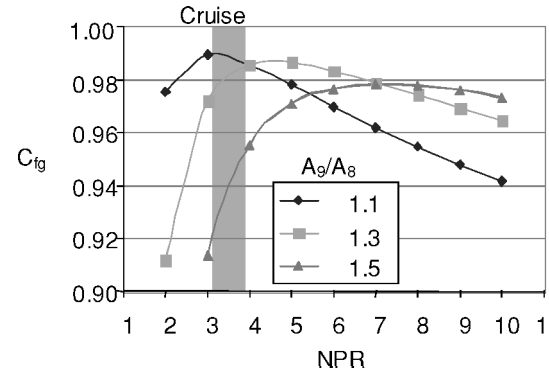

a) A_g = 0.290 m^2

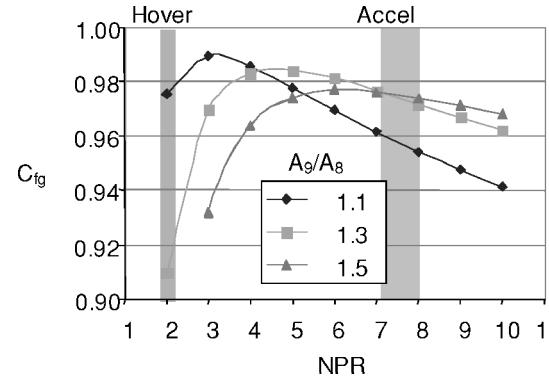

b) A_g = 0.484 m^2

Fig. 2 C_{fg} predictions for various nozzle configurations.

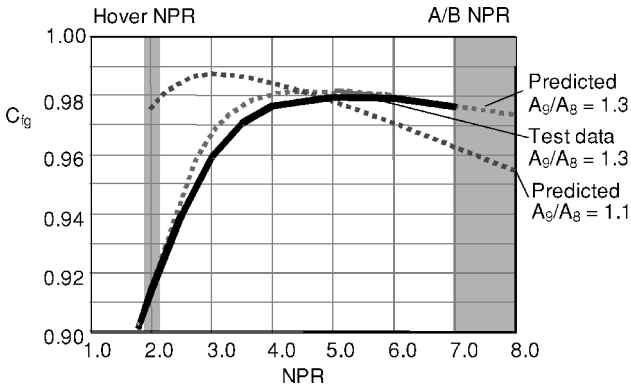

Fig. 3 JSF baseline nozzle test results ($A_8 = 0.484\,m^2$).

resulting in thrust loss and an underexpanded flow. The peak C_{fg} is lower as A_9/A_8 or the divergence angle increases due to a reduction in C_{div}.

Figure 2 shows the three key operating conditions of the JSF. For $A_8 = 0.290\,m^2$, Fig. 2a shows that at cruise, $A_9/A_8 \approx 1.2$ for optimum performance, whereas Fig. 2b shows that for $A_8 = 0.484\,m^2$, $A_9/A_8 \approx 1.3$ is optimum for the afterburning transonic acceleration point with NPR > 6. Increasing A_9/A_8 at this condition does not yield significant gains in performance due to the tradeoff between C_{div} and C_{exp}. At the hover condition (also shown in Fig. 2b), a small area ratio of 1.1 or less is required for optimum performance. This is to be expected because at an NPR of 2 a simple convergent or sonic nozzle would expand the flow to ambient pressure. The dramatic difference in the required A_9/A_8 at afterburning and hover conditions is clearly evident.

Experimental and analytical C_{fg} results for $A_8 = 0.484\,m^2$ and $A_9/A_8 = 1.3$ representing afterburning or hover are shown in Fig. 3. The agreement between test and analysis is about 0.5% of the C_{fg} value. As predicted, the $A_9/A_8 = 1.3$ nozzle provides good performance at afterburning conditions, but exhibits significant overexpansion loss at hover.

Critical combat performance points drive the selection of the area ratio schedule. For $A_8 = 0.290\,m^2$, $A_9/A_8 = 1.2$ is selected to provide high thrust efficiency at cruise. For $A_8 = 0.484\,m^2$, $A_9/A_8 = 1.3$ is selected to give good performance at afterburning conditions. Because the hover condition occurs at $A_8 = 0.484\,m^2$, it also presents $A_9/A_8 = 1.3$, as opposed to the lower, desired value of $A_9/A_8 = 1.1$ required for high C_{fg}. The results of Fig. 2 shows that for the JSF nozzle in hover, the predicted $C_{fg} \approx 0.91$ at $A_9/A_8 = 1.3$ is about 4% lower than that of $A_9/A_8 = 1.1$. A 1% loss in C_{fg} at hover results in a 710 N loss in thrust in the aft nozzle. Because thrust must be balanced about the center of gravity, the thrust of the lift fan must also be adjusted, producing an overall trimmed thrust loss of 1510 N.

Conclusions

Analysis of a STOVL aircraft nozzle in hover showed that there is significant overexpansion loss at hover when $A_9/A_8 = 1.3$. This analysis was supported by cold-flow, subscale tests. At the time of this study, it was determined that the performance was adequate to accomplish the immediate goals of the Concept Demonstration Program.

Acknowledgments

The authors acknowledge the support of Lockheed Martin Aeronautics Company (LMAC) for this study. They also are indebted to Brad Glass, John Richey, and Brant Ginn of LMAC for their technical expertise in the computational fluid dynamics analysis, model design, and test data analysis, respectively.

References

[1]Oates, G. C., *Aerothermodynamics of Gas Turbine and Rocket Propulsion*, rev., AIAA, Washington, DC, 1988, p. 8.

[2]Terrier, D. A., and McFarlan, J. D., "An Investigation of the F-16C/F110 Afterbody Drag and Jet Effects at Transonic Mach Numbers," General Dynamics, Fortworth, Texas, Rept. 16PR4324, April 1985.

[3]Kuchar, A. P., "Variable Convergent–Divergent Exhaust Nozzle," *Aircraft Propulsion Systems Technology and Design*, edited by G. C. Oates, AIAA, Washington, DC, 1989, pp. 305–329.